# HOT TEARING SUSCEPTIBILITY IN DC CAST ALUMINUM ALLOYS

N. Jamaly[1], A.B. Phillion[1], S.L. Cockcroft[2], and J.-M. Drezet[3]

[1]Okanagan School of Engineering, University of British Columbia, Kelowna, Canada
[2]Dept. of Materials Engineering, University of British Columbia, Vancouver, Canada
[3]LSMX, Ecole Polytechnique Fédérale de Lausanne, Lausanne, Switzerland

Keywords: Semi-solid constitutive behavior, microstructure, Direct Chill Casting, Aluminum Alloys, Hot Tearing

## Abstract

Hot tearing and loss of dimensional stability are two key defects related to industrial aluminum alloy casting processes. In order to investigate their occurrence, a new semi-solid constitutive law [20] for AA5182 that takes into account cooling rate, grain size and porosity has been implemented into a Direct Chill casting process model for round billets. The semi-solid stress-strain predictions provided by this new constitutive law as well as the effects of processing parameters were then examined to demonstrate the relationships between defect formation, microstructure, and processing variables.

## Introduction

In aluminum alloy Direct Chill (DC) castings, variable thermal, strain, and strain-rate combinations will spawn abnormally high thermal stresses that result in the formation in several types of imperfections within the cast component. Defects including loss of dimensional stability and hot tearing are two of the main quality concerns related to thermo mechanical behavior. Over the past few decades, a number of models have been developed [1-7] to predict the formation of stresses and strains within the casting, which in turn provides an assessment of when and how these defects can arise. One of the main findings has been the relative importance of processing parameters [8, 9]. Casting speed is believed to be the most important parameter that affects hot tearing defects [9, 10], while pouring temperature and cooling water flow rate are of reduced importance [9].The physical effect of increased casting speed is both an overall increase in the solidification rate, and a proportional increase in the thickness of the mushy zone region [8].

Since early 1970s, numerical models have been used to simulate the DC casting process. The earliest models were simple heat transfer simulations [eg. 5,11]. More recently, complex thermal stress models [e.g. 4, 12, and 13] have been developed which take into account the constitutive behavior of the material in both solid and semi-solid states. The constitutive equations used to describe material behavior in the solid include plastic-strain [14] and creep based power-law equations [15] as well as internal state variable models that includes a term for microstructure evolution [16]. The generally accepted practice is to include the effects of strain hardening and strain rate sensitivity, usually through the use of the so-called modified Ludwik equation,

$$\sigma(T,\varepsilon,\dot{\varepsilon}) = K(T)\left(\varepsilon_p + \varepsilon_{p_0}\right)^{n(T)}\left(\dot{\varepsilon}_p + \dot{\varepsilon}_{p_0}\right)^{m(T)} \quad (1)$$

where *K*, *m*, and *n* are alloy specific and temperature dependent parameters. In Eq.(1), $\sigma$ is the stress (MPa), *K* is a material constant related to the strength of the material (MPa), *n (m)* is the

strain hardening (strain-rate sensitivity) exponent, and $\varepsilon_p(\dot{\varepsilon}_p)$ is the plastic strain (strain-rate, $s^{-1}$). The offset constants $\varepsilon_{p_0}$ and $\dot{\varepsilon}_{p_0}$ are used to circumvent convergence issues.

However, when simulating defect formation such as hot tearing, it is the semi-solid constitutive behavior that is key. Modeling the metallic-alloy semi-solid behavior has always been a challenge because of the large range of viscosity between $0 < f_s < 1$, and the stochastic nature of the solidification process. In the context of DC casting, one successful approach, initiated by Drezet and Eggeler, was to use a modified creep law to describe the semi-solid behavior of AA5182 [17]. In this work, it was assumed that liquid cannot carry any load, which is entirely carried by the existing solid network. This constitutive law was refined by Van Haaften et al. [14] to consider the critical term to be (1- $f_{LGB}$), where $f_{LGB}$ is the fraction of grain boundary area covered by the liquid, instead of the fraction solid, $f_s$. A further refinement, to utilize an internal variable to represent the state of cohesion of the mush, was proposed by Ludwig et al. [18].

A second methodology has been to simply extend the range of Equation (2) up to the temperature corresponding to the fraction solid for mechanical coherency, $T_{coh}$,(e.g. [13,19]), and then to assume a low elastic modulus and high yield stress rheology above this point. Although this methodology is relatively easy to implement in FE and has the advantage of minimizing false strain accumulation in the semi-solid, its main drawback is that there is no link to microstructural features. Recently, a new constitutive equation for semi-solid AA5182 has been proposed by Phillion et al. [20] that takes advantage of the benefits of the Ludwik equation formulation within an FE simulation while also including microstructural features. The reader is referred to [20] for further details of the formulation of this constitutive law, along with its validation. In this law,

$$\sigma\left(f_s, f_p, \bar{d}\right) = f_s \sigma_s \cdot \left(\varepsilon_p + \varepsilon_0\right)^{n(T)} \cdot K_p \cdot \left(1 - \frac{f_p}{1 - f_s}\right) \tag{2}$$

with:

$$\sigma_s = (483.5 - 0.77T)\dot{\varepsilon}^{0.205+0.000\,06T} \tag{3}$$

$$h = \bar{d}\left(1 - {f_s}^{1/3}\right) \tag{4}$$

$$n = -6.35\times10^{-4}h^2 + 0.0202h \tag{5}$$

where $K_p$ is a parameter related to the fraction porosity, $f_p$, $\sigma_s$ is the solid flow stress (MPa) of type elastic-perfectly-plastic, $\bar{d}$ is the average grain size, $h$ is the thickness of the liquid channels between grains, and $n$ is a strain hardening parameter related to the grain size of the solid skeleton. The phenomenological expression for $n$ has been determined based on a regression analysis of semi-solid tensile deformation experiments and microstructure simulations. In the current work, the constitutive law presented in Eqs. (2)-(5) has been implemented into a previously-developed DC casting model for Al alloy round billets [21].Stress-strain predictions from a series of simulations were then analyzed with respect to the casting speed, grain size and different coherency temperatures. These results were used to investigate the effects between casting parameters, microstructure and hot tearing in DC castings.

## Model Formulation

Finite Element Modeling

The DC casting process for AA5182 was simulated using the commercial FE package ABAQUS – v6.10. The computational domain was assumed to be axi-symmetric, and the simulations were conducted in the usual way in which layers of elements of a given thickness are added to the

domain at regular time intervals corresponding to the casting speed. In total, 100 layers of elements were used, each 11 mm thick. The initial condition was the pouring temperature. The boundary conditions account for primary cooling through the mold, air gap formation, and secondary cooling where the water hits the billet and flows along its surface. The bottom of the billet was cooled using a constant heat flux of 1000 W/m$^2$ to simulate heat transfer between the billet and the bottom block. Further details on these boundary conditions can be found in [21].

Thermophysical Properties

The specific heat, latent heat, density, and thermal conductivity of the AA5182 alloy, along with the Young's modulus and the coefficient of thermal expansion (CTE) used in the current study were taken from [22]. The solidification path of the alloy was taken from the work of Thompson et al. [23], with liquidus and solidus temperatures of 523˚C and 637˚C respectively. To properly simulate the DC casting process, the thermophysical properties need to include the change in behavior occurring during solidification, specifically, the variation of Young's modulus and CTE that occurs with increasing fraction solid. The approach utilized by Drezet [13], is reproduced in the current model. As shown in Table 1, this approach considers that the Young's modulus and CTE are only of significant value below $T_{coh}$, whereas above they are reduced to a small value.

Mechanical Behavior

The mechanical behavior of the AA5182 alloy during the DC casting process was integrated within the ABAQUS FE package using the UHARD subroutine. At temperatures corresponding to the fully solid state, the mechanical behavior of the AA5182 material was modeled as an elasto-plastic material using the modified Ludwik formulation as per Alankar et al. [24] and shown in Table 1. At temperatures in the range $T_{solidus}<T<T_{coh}$, the constitutive law shown in Eqns.(2)-(5) was utilized to include the effects of $\bar{d}$ on semi-solid deformation. Although this law also includes the effects of $f_s$ and $f_p$, this variation in these parameters in different regions of the casting is not taken into account in this initial study (i.e. (a) $f_p$ is assumed to be 0 and hence $K_p$=1 [21], and (b) the cooling-rate effects on the evolution of fraction solid with temperature are ignored). At temperatures above $T_{coh}$, the mechanical behavior was considered elasto-plastic with a small yield stress and independent of strain rate. This assumption is used to ensure a low level of stress in the region of the semi-solid where hot tearing does not occur. The resulting semi-solid stress-strain relationships for AA5182 are presented graphically in Figure 1.

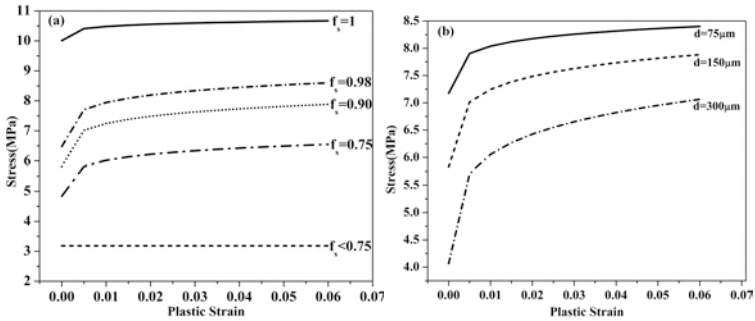


Figure 1: Graphical representation of the semi-solid stress-strain relationship after Eqns.(3)-(6) showing (a) the effect of $f_s$ at $\dot{\varepsilon}= 10^{-3}\ s^{-1}$and $\bar{d}$= 150 μm, and (b) the effect of $\bar{d}$ at $f_s$ = 0.90.

Table 1: Mechanical Behavior AA5182 (Temp. given in Celsius)

| | $T_{25^\circ C}<T<T_S$ | $T_S<T<T_{coh}$ | $T_{coh}<T<T_L$ |
|---|---|---|---|
| $\alpha$ ($^\circ C^{-1}$) | $-0.0235+2x10^{-5}T+4x10^{-8}T^2$ | -same- | 0 |
| $E$ (GPa) | $-0.162T^2 + 7.52T + 71589$ | $100.836 - 0.174T$ | 0.01 @$T=T_{coh}$ +5K |
| $\sigma$ (MPa) | See Reference [24] | Eqns. (2)-(5) | $\sigma_y = \sigma_y^{coh}$ |

**Results and Discussion**

Below, the semi-solid microstructure state along with the stress-strain predictions are provided in order to investigate the link between microstructure, processing parameters, and hot tearing. From a processing standpoint, the microstructural features taken into account in Eqns.(2)-(5) are related to the casting speed and the cooling water flow rate. Both of these processing parameters will modify the local fraction solid, grain size, and porosity for a given alloy composition. The cooling rates experienced by the billet during solidification are shown in Figure 2(a) for a typical casting velocity of 66 mm / min. The cooling rate has been calculated as follows,

$$\dot{T} = \frac{T_{coh} - T_{liq}}{\Delta t} \qquad (6)$$

where $\Delta t$ is the time difference between the liquidus and coherency temperatures. This averaged cooling rate was used since it provides a measure of the variation in billet cooling conditions that define the microstructure state at the start of the coherency regime. The contour plot shown in Figure 2 reveals that although the highest cooling rate is achieved near the casting surface, there is not a large difference between the surface and centerline solidification rates using the definition shown in Eq.(6) as all values are in the range of -1˚C/s. Thus, in inoculated commercial aluminum alloys, such as AA5182, the grain size will be similar throughout the casting. A study of DC cast Al-Cu alloys [25] confirms this hypothesis, and has also shown that an increase in casting speed results in substantial grain refinement over the entire cross-sectional area, as well as a ceasing of grain coarsening close to the billet center. In Figure 2(b), the cooling rate over the final solidification regime (i.e. $T_{coh}<T<T_{sol}$) has been presented. In comparison to Figure 2(a), the solidification rates are now quite different between the surface and the center, since solidification occurs rapidly once the water sprays begin to cool the surface of the billet

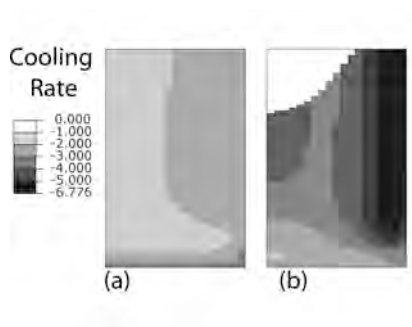


Figure 2: Cooling-rate contour plots over the range (a) [$T_{liq}$, $T_{coh}$] and (b) [$T_{coh}$, $T_{sol}$] over the first 300 mm of cast length.

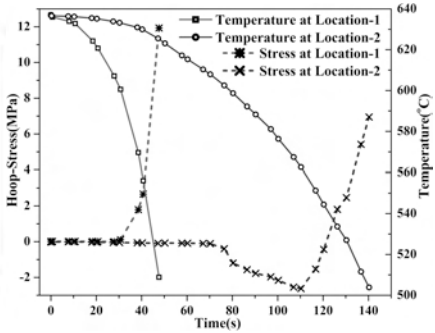


Figure 3: Evolution in $\sigma_{Hoop}$ and $T$ with time; $t$=0s corresponds to $T_{liq}$ at each location.

whereas the centerline remains in the mushy state for the longest time and thus is prone to hot tearing. The highest cooling rates in this range are on the order of -6˚C/s. Note that the large white area in the upper left-hand corner of Figure 2(b) has not yet reached the $T_{sol}$.

The FE simulation can be used to provide a detailed description of the evolution of stresses, strains, and temperature during the casting process. The predicted evolution in hoop stress and temperature at two locations within the billet have been chosen for comparison and shown in Figure 3. Location 1 is 44 mm above the bottom block and on the centerline while Location 2 is at the same height but just below the casting surface. The hoop stress is shown since it is considered to be the major driving force for hot tearing initiation. As can be seen from the figure, the cooling curves are significantly different throughout the entire solidification regime with Location 1 cooling in 15 s compared to 65 s at Location 2, owing to the water-cooling at the surface of the billet. At Location 2, the hoop stress is seen to be tensile throughout the entire solidification regime, increasing to 4 MPa at the solidus, while at Location 1 the stress is initially compressive but then evolves to tensile at the end of the solidification regime. This variation of thermal stresses arises from the differential cooling conditions at these two locations.

The variation in the predicted hot tearing strain accumulated in the brittle transition region ($\Delta\varepsilon_{HT}BTR$) and hoop stress at $f_s$ = 0.98 as a function of distance above the bottom block at the centerline of the billet is shown in Figure 4 for three different grain sizes, $\bar{d}$ = 75, 150, and 300 μm at a casting speed of 66 mm/min and a coherency temperature of 602˚C (i.e. $f_{s,coh}$ = 0.75). Here the hot tearing strain is assumed to be the component of strain in a direction perpendicular to the direction of heat flux in the solid-liquid interface [26]. Furthermore, only the strain accumulated between the coherency temperature and $f_s$=0.98 is considered, as shown below,

$$\varepsilon_{HT} = \varepsilon_{rr} sin\gamma - \varepsilon_{zz} cos\gamma + \varepsilon_{\theta\theta} \quad (7)$$

$$\Delta\varepsilon_{HT}BTR = \varepsilon_{HT}(f_s = 0.98) - \varepsilon_{HT}(f_s = f_{s,coh}) \quad (8)$$

where, $\varepsilon_{rr}$, $\varepsilon_{zz}$ and $\varepsilon_{\theta\theta}$ are the strains in the radial, axial and hoop directions, and $\gamma$ is the angle between the heat flux and $\varepsilon_{rr}$. Unfortunately, the relationship between cooling rate and grain size has not yet been established in this alloy. Additional simulations were also conducted using a slower casting speed (40 mm/min) and a lower coherency temperature (580˚C, i.e. $f_{s,coh}$ = 0.90). The value of $f_s$ = 0.98 was chosen since the grains will have mostly coalesced to the point where the solid will form a continuous skeleton with a mechanical strength close to that of the solid.

As can be observed from Figure 4(a), the relevant strain is compressive for the first 100 mm of casting, but gradually shifts to a tensile value and is very large at approximately 150 mm from the bottom block. Industrially, this is the region of the billet where hot tears are known to initiate. The strains are smallest when a slow casting speed of 40 mm/min is used since there is a smaller thermal gradient and hence a smaller differential thermal contraction at low cooling rates. Actually, the strain for this slow casting speed really does not shift to the tensile region at all. The effect of grain size is somewhat counterintuitive. Although, as shown in Figure 1, the semi-solid strength increases with decreasing grain size, the centerline of the casting is more deformed using the smaller grain sizes. This counterintuitive result is obtained since the metal close to the centerline is the last to solidify and thus as the metal around this region is cooler, it also has higher strength with a smaller grain size. So, all the stresses are transferred to the weak semi-solid and consequently a higher strain is observed. The effect of coherency temperature is a shift

in the strain further away from the bottom block when the coherency temperature is reduced to 580˚C. The variation in hoop stress shown in Figure 4(b) corroborates this analysis. As expected, the hoop stress is tensile, with slower casting speeds and lower coherency temperature generating smaller hoop stresses as predicted by Figure 1. The effect of grain size on stress is minimal. Another important issue in Figure 4 is the variability in the predicted strain. This fluctuation is due to the addition of the layers of elements at each time step, which causes a sudden change of stiffness in the model domain and consequently the strains oscillate. Neglecting this issue, the important trends can still be observed.

The variation in $\Delta\varepsilon_{HT}BTR$ and hoop stress at $f_s$ = 0.98 as a function of distance from the centerline of the casting at 143 mm above the bottom block is shown in Figure 5 using the same five simulation conditions as in Figure 4. As can be seen in Figure 5(a), $\Delta\varepsilon_{HT}BTR$ is tensile in close to the centerline and gradually becomes compressive towards the surface in all five cases.

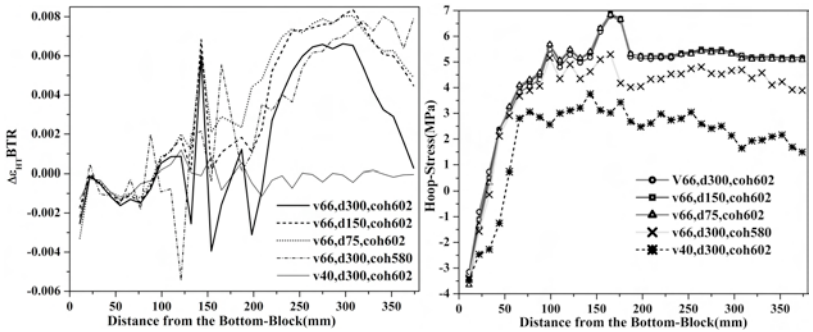


(a) (b)

Figure 4: Variation in the predicted (a) hot tearing strain and (b) hoop stress at $f_s$ = 0.98 as a function of distance from the bottom block and at the centerline of the casting.

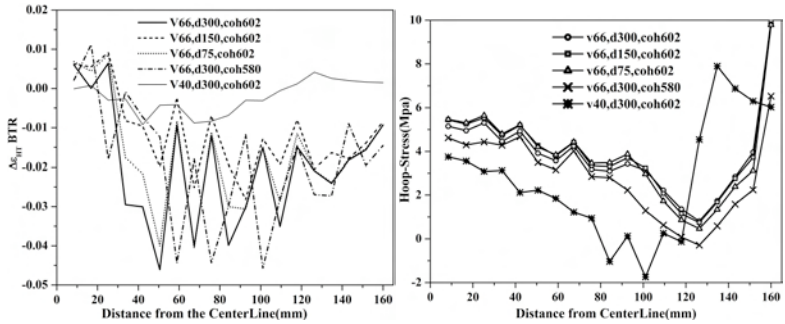


(a) (b)

Figure 5: Variation in the predicted (a) hot tearing strain and (b) hoop stress at $f_s$ = 0.98 between the centerline and the surface of the billet at 143 mm above the bottom block.

The highest tensile strain is obtained at approximately 30 mm from the centerline. This high tensile stress region is most prone to hot tearing. In the compressive regime, the strains also oscillate because of the layer additions. Similar trends are seen in Figure 5(a) as discussed with respect to Figure 4, i.e. the predicted semi-solid deformation is strongly affected by casting speed and moderately affected by the grain size. Furthermore, the strain is largest in the simulation using $T_{coh}$ = 580˚C because the semi-solid material remains quite weak until this temperature is achieved. Thus, as the outer parts of the billet cool and contract, the center will deform in tension. In terms of the hoop stress, it can be seen in figure 5(b) that the centerline is under tensile load, which then transitions to compressive further out. The surface load is strongly tensile because of the high heat flux boundary condition cooling the billet. The billet cast using the slower casting velocity experiences a lower centerline tensile loading because the corresponding thermal gradient is quite low.

## Conclusions

A new semi-solid constitutive model that takes into account microstructural features has been successfully incorporated into a FE simulation of the Direct Chill casting of AA5182 aluminum alloy billets. Based on an analysis of a series of simulations under different microstructural and processing conditions, the following conclusions can be drawn:

1. The equivalent plastic strain is highest at the centerline of the billet, and decreases towards the surface. Similarly, the strain increases with increasing distance from the bottom block.
2. The choice of the coherency temperature has a major influence on the evolution of stresses and strains with the DC cast structure. A higher coherency point results in decreased semi-solid plastic strains and increased tensile stresses.
3. Under identical cooling conditions, a lower casting speed results in reduced semi-solid strains. Thus, a decrease in casting speed should reduce the vulnerability of the cast structure to hot tearing defects as reported industrially.
4. Grain size plays an important role in quantifying semi-solid deformation and hence hot tear formation. The total accumulated semi-solid plastic strain and grain size are inversely related with strain decreasing with increasing grain size. Conversely, there appears to be little variation in stress due to grain size effects.

## References


1. Drezet, J.-M., and Rappaz, M. 1996. Modeling of ingot distortions during direct chill casting of aluminum alloys.*Metall. Mater. Trans.* 27A, p.3214-3225.
2. Drezet, J.-M., and Rappaz, M. 1997. Direct Chill casting of aluminum alloys: Ingot distortions and mold design optimization. In Huglen R.,ed.,Light Metals, TMS. 1071-1080.
3. Drezet, J.-M., Burghardt, A., Fjaer, H. G., andMagnin, B. 2000. Thermomechanical effects in DC casting of Al. alloy: A numerical benchmark study. *Solidif. &Grav*.p.493-499.
4. Fjær, H., Mo, A. 1990. Alspen - a mathematical model for thermal stresses in direct chill casting of aluminium billets. *Metall. Mater. Trans.* 21B, p.1049–1061.
5. Moriceau,J. 1975.Thermal Stresses in DC Casting of Al Alloys. In Rentsch R.,ed., Light Metals, TMS, 119-133.
6. Nedreberg, M. L. 1991. Thermal stress and the hot tearing during the DC casting of AlMgSi billets. *PhD thesis*, University of Oslo.

7. Sengupta, J., Cockcroft, S. L., Maijer, D. M., Wells, M. A., and Larouche, A. 2004. On the development of a 3D thermal model to predict cooling during the start-up of the direct chill-casting process for an AA5182 Al alloy ingot. *Metall. Mater. Trans.* 35B, p.523-540.
8. Emley, E.F. 1976. Continuous Casting of Aluminum. *Intl. Metals Reviews* 206, p.75-115.
9. Nagaumi, H., Aoki, K., Komatsu, K., and Hagisawa, N. 2000. Internal crack in DC casting billet of high strength Al-Mg-Si alloys. Aluminum Alloys: Their Physical and Mechanical Properties - Pts(1-3), 331-3, p.173-178.
10. M'Hamdi, M., Kieft, R., Mortensen, D. Mo, A. and Rabenberg, J. 2002. Effect of increasing the casting speed on hot tearing formation for a DC cast 3xxx alloy. *Al.* 78, p.847–851.
11. Weckman,D.C., and Niessen,P.1982, A numerical simulation of the D.C. continuous casting process including nucleate boiling heat transfer.*Metall. Trans.* 13B, p.593–602.
12. Drezet, J.-M., Rappaz, M., and Krahenbuhl, Y. 1999. Modelling of thermomechanical effects during direct chill casting of AA1201. Aluminum Alloys: Their Physical and Mechanical Properties - Pts(1-3), 217, p.305-310.
13. Drezet, J.-M., and Phillion, A.B. 2010. As-cast residual stresses in an aluminum alloy AA6063 billet: Neutron diffraction measurements and finite element modeling.*Metall. Mater. Trans.* 41A, p.3396-3404.
14. Haaften,W.M.V., B. Magnin,B., Kool,W.H. and Katgerman, L. 2002. Constitutive behavior of as-cast AA1050, 3104, and 5182. *Metall. Mater. Trans.* 33A, p.1971–1979.
15. Farup, I., and Mo, A. 2000. The effect of work hardening on thermally induced deformations in aluminum DC casting. *J. Thermal Stresses*. 23, p.71-89.
16. Mo, A., and Holm, E. J. 1993. On the use of constitutive internal variable equations for thermal-stress predictions in aluminum. *Modell. Id. & Ctrl.* 14, p.43-58.
17. Drezet, J. M., and Eggeler, G. 1994. High apparent creep activation-energies in mushy zone microstructures. *Scr. Metall. Mater.* 31, p.757-762.
18. Ludwig, O., Drezet, J., Martin, C., and Suery, M. (2005). Rheological behavior of al-cu alloys during solidification: Constitutive modeling, experimental identification, and numerical study. *Metall. Mater. Trans.* 36A, p.1525-1535.
19. Sengupta, J., Cockcroft, S., Maijer, D., & Larouche, A. (2005). Quantification of temp., stress, and strain during the start-up phase of direct chill casting process by using a 3D fully coupled thermal and stress model for AA5182 ingots.*Mater. Sci. Eng. A.* 397, p.157-177.
20. Phillion, A. B., Cockcroft, S. L., and Lee, P. D. 2009. Predicting the constitutive behaviour of semi-solids via a direct finite element simulation: Application to AA5182. *Modell. Simul. Mater. Sci. & Engr.* 17:055011.
21. Drezet, J.-M., Rappaz, M., Grun, G., and Gremaud, M. 2000. Determination of thermophysical properties and boundary conditions of direct chill-cast aluminum alloys using inverse methods. *Metall. Mater. Trans.* 31A, p.1627-1634.
22. Mondolfo, L. F. 1976.Aluminum Alloys: Structure&Properties, Butterworths, London, UK.
23. Thompson, S., Cockcroft, S., and Wells, M.A. 2004. Effect of cooling rate on solidification characteristics of aluminium alloy AA 5182. *Mater. Sci. &Techn.* 20, p.497-504.
24. Alankar, A., and Wells, M. A. 2010. Constitutive behavior of as-cast aluminum alloys AA3104, AA5182 and AA6111. *Mater. Sci. Eng. A.* 527, p.7812-7820.
25. Suyitno, A., Eskin, D. G., Savran, V. I., and Katgerman, L. 2004. Effects of alloy composition and casting speed on structure formation and hot tearing during direct-chill casting of Al-Cu alloys. *Metall. Mater. Trans.* 35A, p.3551-3561.
26. Drezet, J.-M. and Rappaz, M. 2001. Prediction of hot tears in DC-cast aluminum billets. In Anjier, J., ed., Light Metals, TMS, 887-893.